Measurements of H_2O broadened by CO_2 line-shape parameters

Ducreux; Grouiez, B.; Robert, S.; Lepère, M.; Vispoel, B.; Gamache, R. R.; Régalia, L.

Published in:
Journal of Quantitative Spectroscopy and Radiative Transfer

DOI:
10.1016/j.jqsrt.2024.109026

Publication date:
2024

Document Version
Peer reviewed version

Measurements of H_2O broadened by CO_2 line-shape parameters: beyond the Voigt profile

É. Ducreux[1,2,3], B. Grouiez[1], S. Robert[2], M. Lepère[3], B. Vispoel[3], R.R. Gamache[4], L. Régalia[1,*]

[1] *Université de Reims Champagne-Ardenne, CNRS, GSMA, Reims, France*

[2] *Planetary Atmospheres, Royal Belgian Institute for Space Aeronomy, 3 Avenue Circulaire, 1180 Brussels, Belgium*

[3] *Research Unit Lasers and Spectroscopies (LLS), Institute of Life, Earth and Environment (ILEE), University of Namur (UNamur), 61 rue de Bruxelles, Namur, B-5000, Belgium*

[4] *Department of Environmental, Earth, and Atmospheric Sciences, University of Massachusetts Lowell, 1 University Avenue, Lowell, MA 01854, USA*

Highlights

- New water vapor spectra broadened by CO_2 recorded with a Bruker IFS 125 HR at room temperature in 2.7 µm spectral region

- Retrieval of line parameters with multispectrum fitting procedure

- Use of different beyond-Voigt line profiles (Rautian, quadratic Speed-Dependent Voigt, quadratic Speed-Dependent Rautian)

- Comparison of line collisional parameters with literature

Keywords:

High resolution infrared spectroscopy - Line shape parameters - Water vapor - Carbon dioxide - Line profiles - Planetary atmospheres

Number of pages: 15

Number of figures: 5

Number of tables: 4

* Corresponding author:

E-mail address: laurence.regalia@univ-reims.fr (Laurence Régalia).

Tel.: +33 326 913 319; fax: +33 326 913 147.

Abstract

H_2O is an important molecule in the quest to better understand the evolution of solar system. In the study of Venus and Mars CO_2-rich atmospheres (around 96% of their composition) and because of the space instruments constant improvements, the planetary community needs spectroscopic data as accurate as possible.

Continuing from our previous study [JQSRT 231, 126(2019)], new spectra of H_2O perturbed by CO_2 were measured with our new experimental set-up in the 2.7 µm region to compare with the previous results. After the improvement in the determination of the partial pressure of water vapor, the line parameters were then determined with a multispectrum fitting procedure using a Voigt profile in the same way as in [JQSRT 231, 126(2019)]. This led to characteristic W-shape residuals that have been improved using beyond-Voigt profiles. Our investigation showed that considering the speed dependence of collisional line parameters is essential to obtain better line-shape parameters in the considered experimental conditions.

1. Introduction

As part of the study of our solar system evolution and research on terrestrial water's origins, it is particularly important to know the distribution of water vapor and its isotopologues in the atmosphere of our planetary neighbors, Venus and Mars. Venus Express (2008-2014) and ExoMars Trace Gas Orbiter (2016-), both ESA missions and also ground-based measurements have mapped water [1-7]. From these measurements, the isotopic ratio, deuterium to hydrogen, D/H, has been deduced to constrain atmospheric evolution scenarios [8-11].

Until recently, collisional parameters of H_2O broadened by air were used due to lack of data instead of H_2O broadened by CO_2 line collisional parameters in planetary spectrum analysis. It was therefore essential to provide the planetary science community with measurements of H_2O broadened by CO_2 line-shape parameters in several regions of atmospheric interest. Some studies have already contributed to the determination of these collisional parameters [12-20] for H_2O and [21-24] for HDO. Note, to our knowledge, CO_2-broadening parameters of D_2O have never been measured. Among these studies, **Reference 12** presented spectra recorded in the 2.7 and 6 µm regions with a step-by-step Connes' type Fourier-Transform spectrometer (FTS) and analyzed with a Voigt profile. More recently new spectra were measured in the 2.7 µm region with a Bruker IFS 125 HR FTS coupled to a 2-meter White-type cell. The pressure of water vapor was kept sufficiently low to avoid self-broadening contribution, as was already done in our previous study [12]. As water vapor is a polar molecule, it is well-known that the sample adsorption must be considered. So, the H_2O partial pressure needs to be determined precisely. The differences between observations and the modeling (i.e. the residuals) showed that the partial pressure of water vapor in the experiment may not have been considered properly. Another gas injection method was tested. In [12], an initial mixture of H_2O – CO_2 was injected in the cell and one spectrum was measured after each pumping. Whereas in this work, after the injection of a low pressure of water vapor, the CO_2 was injected gradually, and a spectrum was recorded after each new mixture. The analysis of these new measurements required to go beyond the Voigt profile. Using this common profile led to W-shape residuals due to a narrowing effect. More complex line profiles were investigated to obtain more accurate collisional line parameters.

Section 2 describes the experimental setup and the method for line parameters' retrieval. **Section 3** is dedicated to comparisons and results.

2. Experimental conditions

2.1 Spectra measurements

A FTS, commercial Bruker IFS 125 HR, was used to measure water vapor broadened by carbon dioxide spectra in the 2.7 µm region at room temperature. The wavelength range was selected to be able to compare to previous measurements [12]. The characteristics of the FTS are listed in **Table 1**. During the experiment, a primary oil pump and a turbomolecular secondary pump maintained the absorption path under vacuum - around 5.10^{-5} mbar - to reduce residual background water.

Table 1

A 2-meters White-type cell in stainless-steel was combined with the spectrometer to reach absorption path lengths from 8 to 104 meters.

For the cell pressure monitoring, three thermalized Leybold CTR101N Baratron gauges heads with a range of respectively 10, 100 and 1,000 Torr were used, coupled with a conversion box for pressure reading. They have an accuracy of 0.2% and are calibrated beforehand. Temperatures were measured in the cell by four TCSA Pt100 probes with 0.6 K of accuracy, coupled with a Meilhaus Electronics conversion box.

Experimental conditions are given in **Table 2** for a series of spectra shown in **Figure 1**. The partial pressure of H_2O was 1.465 Torr. Within these conditions, line intensities from 4.10^{-21} to 1.10^{-23} cm^{-1} / (molecule cm^{-2}) were measured in the 2.7 µm region, choosing to analyze lines ranging from 15 to 80% of absorption. As seen in **Figure 1,** by increasing the partial pressure of CO_2 in the cell, the water vapor lines were increasingly broadened, hence the maximum path difference (MPD) was reduced (see **Table 2**) to maintain a good signal to noise ratio with a shorter measurement duration. This led to reach a mean signal to noise ratio around 3500, determined with Bruker's software Opus by selecting several spectral intervals without visible lines. The CO_2 gas was purchased from Air Liquid with a stated purity (CO_2 N48) of 99.998%. The gas injection method is discussed in **Section 2.2.1**.

Table 2

Figure 1

2.2 Line parameters retrieval

A multispectrum fitting procedure was used to determine collisional parameters of H_2O broadened by CO_2 lines. Two software packages were used complementarily. The first one called MultiFiT [25] - MFT - was developed in-house. The second one called MultiSpectrum Fitting - MSF - is described in [26]. Both can fit simultaneously several parameters, such as position, intensity, broadening and shift coefficients, but only MFT enables one to fit the partial pressure. However, MSF is not limited to the Voigt profile and offers more complex line profiles.

The analysis was carried out only on isolated lines with an absorption between 15 and 80% to ensure well defined parameters without any saturation effect.

2.2.1 Gas mixture

Using both the MFT [25] and MSF [26] software with a Voigt profile on absorption lines, signatures on observed - calculated residuals as shown on **Figure 2** (left panel) were observed. This type of residuals differs from the typical W-shape signature generally induced by an inadequate line profile. In our case, the residuals are off-centered suggesting an uncertainty on the water vapor partial pressure. This possibility was investigated and developed further in the next sections.

First, the water vapor was produced by pumping over a sample of liquid water in natural abundance. The use of a static setup for water is quite tricky. H_2O being a polar molecule, it can easily stick on stainless-steel cell walls, because of the adsorption effect. That is why our partial pressure does not correspond to the pressure injected. Therefore, the way the gas mixture is injected will have an impact on the spectra. Indeed, in Ref [12], the water vapor was injected, before adding a single 500 Torr

pressure of CO_2 in the cell. The mixture was then pumped to reach lower pressures. So, the partial pressure of H_2O was different for each spectrum.

For this work, the procedure of gas injection was modified to have the same H_2O partial pressure for each spectrum of a series. Before each new recording, adequate time was taken to allow the mixture to become homogeneous and the pressure to stabilize. With this method, the pressure of H_2O was stable, whereas the mixing ratio changed radically between the four spectra (see **Table 3**).

As our experimental gas injection facility is static and not based on a constant flow that avoids the sticking of water molecules to cell walls [27], a post-correction of the water vapor partial pressure needs to be performed to take into account adsorption [28]. It was then necessary to better determine the H_2O partial pressure to obtain the best fit residuals and line parameters. Our method consisted in fitting the H_2O partial pressure with the MFT software [25] by fixing the intensity values at those of HITRAN2020 [29] on 14 isolated lines. Among these, eleven lines have a relative uncertainty of less than 1%, while the three others have a relative uncertainty between 2% and 5%. This results in a maximum relative uncertainty of approximately 1.9% (weighted mean) for the selected intensities.

It was found that for the 100, 200 and 300 Torr spectra, the fitted H_2O partial pressure was always around 3% lower than the measured one, as seen in **Table 3**. For the 500 Torr spectrum, the fitted pressure had an aberrant value probably coming from the large broadening of the lines and which did not allow convergence to a coherent fitted pressure value. Thus, by considering that the deviation remained constant, the mean of the three first H_2O partial pressures was used for the 500 Torr spectrum. **Figure 2** (right panel) shows a finer improvement of the residuals and clear W-shape signature due to the use of an inappropriate profile.

Table 3

Figure 2

2.2.2 Line profiles and collisional line parameters

The common profile used to fit spectral lines and provided to spectroscopic databases is the Voigt profile (VP) [30], but several studies [31-34] (non-exhaustive list) have already shown that it is not the most suitable for H_2O studies and that it usually can bring a W-shape in the fit residuals coming from a narrowing of the line. To correctly model the lines, other more elaborate line profiles were developed that include physical mechanisms of broadening. The MSF software [26] allows the use of the Rautian profile (RP) [35], the quadratic Speed-Dependent Voigt profile (qSDVP) [36-41] and the quadratic Speed-Dependent Rautian profile (qSDRP) [42]. The VP, RP and qSDVP are limiting cases of the qSDRP [43, 44], as shown in **Table 4**.

Table 4

The Rautian profile takes into account the Dicke narrowing effect [45] due to collision-induced velocity changes in the case of hard collisions. In this model, active light molecules are colliding in a heavy molecule environment at a pressure sufficiently low that the Maxwell-Boltzmann distribution is not maintained. Each new collision causes a speed change, independent of the initial speed of the

molecule. And because it is more likely that a molecule will lose speed after a collision rather than gain it, the Doppler shift decreases and the line narrows.

The quadratic speed-dependent Voigt profile allows to consider the speed dependences of the line width and shift (**Equation 1**) [43] by taking into account the relative speed between the absorbing and the perturbing molecules, which leads to a narrowing and an asymmetry of the line.

$$\begin{cases} \Gamma(v) = \Gamma_0 + \Gamma_2 \left[\left(\frac{v}{v_p} \right)^2 - \frac{3}{2} \right] \\ \Delta(v) = \Delta_0 + \Delta_2 \left[\left(\frac{v}{v_p} \right)^2 - \frac{3}{2} \right] \end{cases} \quad (1)$$

Γ_0 and Δ_0 are respectively the averaged values over all molecular speed v of the line collisional width and shift. Γ_2 and Δ_2 are respectively the quadratic speed dependence of the line collisional width and shift. $v_p = \sqrt{2k_BT/m}$ is the most probable speed at temperature *T* of the active molecule of mass *m*.

The quadratic dependence model [38, 39] is a good approximation allowing a relatively short time of numerical computation.

Finally, the quadratic speed-dependent Rautian profile is a combination of two profiles mentioned above considering the confinement narrowing effect and the speed dependence of the broadening and shift coefficients. It results in a longer calculation time compared to that of the qSDV profile.

3. Results and discussion

In this section, the results obtained with the four spectra of the series given in **Table 2** were presented. As the partial pressure of H_2O was previously determined (see previous section) with the MFT program [25], the line intensity was fixed during the fitting procedure; the position, the CO_2 broadening and shift coefficients were adjusted. The following results were obtained using the MSF software [26].

3.1. Comparisons using Voigt profile

First, in **Figure 3** the CO_2 broadening coefficients coming from our previous study [12] were compared with those obtained in this work (called "*S2023*" from now on), all determined with a Voigt profile. Followed mean relative deviations were found: 2.8% between the experimental coefficients from spectra recorded in 2023 with and without water vapor pressure correction and 2.3% between the experimental coefficients from [12] and *S2023* with pressure correction. Between MCRB calculations provided in [12] and *S2023* with pressure correction, only 2.0% were obtained against 4.1 in [12] for the same selected lines. So, making a correction to the water vapor partial pressure helped to obtain a better agreement between the experiments and the calculations. The plot was made with respect to the index J''*(J''+1)+Ka''-Kc''+1, which is unique for each line.

Figure 3

3.2. Line profile comparisons

After the correction of the water vapor partial pressure on our spectra, there remained a W-shape on our residuals, typical of the Voigt profile model (**Figure 2**, right panel). To go beyond, more complex line profiles, described above, were used: the Rautian profile, the quadratic Speed-Dependent Voigt profile and the quadratic Speed-Dependent Rautian profile. An example of the fit residuals obtained using the four different line profiles is shown in **Figure 4**.

Figure 4

Considering firstly the Dicke narrowing effect using the Rautian profile, **Figure 4** shows that it did not bring significant improvement. In contrast, the residuals are really improved by a factor of at least five if the speed-dependence on CO_2-broadening and CO_2 pressure-induced coefficients are considered using the quadratic Speed-Dependent Voigt profile. The W-shape, previously visible, was greatly diminished. Using quadratic Speed-Dependent Rautian profile led to residuals like those obtained with the qSDVP.

The quadratic Speed-Dependent Voigt and the quadratic Speed-Dependent Rautian profiles were more suitable than the other models to obtain very low residuals. And because the first had a lower computation time and a lower number of parameter than the second for similar results, the quadratic Speed-Dependent Voigt profile seems to be in the considered experimental conditions, the best choice in the analysis of H_2O broadened by CO_2 lines.

3.3. Literature comparison

By comparing our CO_2 broadening coefficient measurements obtained with the quadratic Speed-Dependent Voigt profile with those obtained with the Voigt profile, a mean relative deviation of approximately 4.1% has been found for 78 transitions in ν_1, $2\nu_2$ and ν_3 bands. A similar observation was done in [17], where the broadening for the quadratic speed-dependent Voigt profile was found higher of 4.7 % for $\nu_1+ 2\nu_2+ \nu_3$, $2\nu_1+ \nu_3$ and $3\nu_1$ bands, than broadening for Voigt profile.

In the literature, the only study at 2.7 µm using a profile considering the speed is the work of Deichuli et al. [18]. Since in our study, a cell with a longer path length was used (8 m compared to 24 cm), these two studies did not have access to the same transitions. However, 18 lines were common with our measurements and comparisons are presented in **Figure 5**. The mean relative deviation for CO_2 broadening coefficients and their speed dependence was found of, respectively of 0.6% and 15.3%. So, a good agreement was found for the first parameter and quite far for the second one with no clear explanations. Nevertheless, it was not surprising given that the speed dependence coefficients are difficult to determine. Note that in [18], the speed-dependence of the shift induced by the CO_2 pressure was fixed to zero whereas it was not the case in this work. By using the same configuration in our study, the mean relative deviations for CO_2 broadening coefficients and their speed dependence are larger, respectively 1.3% and 33.6%.

Figure 5

4. Conclusions

An IFS 125 HR Bruker Fourier-Transform spectrometer was used to measure spectra of H_2O broadened by CO_2 in the 2.7 µm spectral region of atmospheric interest. A multispectrum fitting procedure was used to better determine the water vapor partial pressure. The line-shape parameters were determined with several line profiles: Voigt profile, Rautian profile, quadratic speed-dependent Voigt profile and quadratic speed-dependent Rautian profile and their fit residuals compared. The quadratic speed-dependent Voigt profile was the more appropriate line profile to fit H_2O broadened by CO_2 spectral lines yielding low residuals. This work is a part of an ambitious investigation aiming at preparing future space missions. Spectral regions of interest for Ariel [46,47] and EnVision [48], for instance, will be studied.

Acknowledgements

This work was supported by the Programme National de Planétologie (PNP) of CNRS-INSU co-funded by CNES. S.R. acknowledges funding by the Belgian Science Policy Office (BELSPO) through the FED-tWIN program (Prf-2019-077 - RT-MOLEXO) and through financial and contractual support coordinated by the ESA Prodex Office (PEA 4000137943, 4000128137). B.V. would like to thank the F.R.S.-FNRS for postdoctoral financial support. The authors sincerely thank Dr K. Sung from Jet Propulsion Laboratory in California (USA) for many useful discussions, his expertise and advice on pressure measurements of water vapor.

References

[1] de Bergh, C., Bézard, B., Crisp, D., Maillard, J.P., Owen, T., Pollack, J., Grinspoon, D.H., 1995. Water in the deep atmosphere of Venus from high-resolution spectra of the night side, Adv. Space Res. 15, 79-88. https://doi.org/10.1016/0273-1177(94)00067-B

[2] Fedorova, A., Korablev, O., Vandaele, A.C., Bertaux, J.-L., Belyaev, D., Mahieux, A. , Neefs, E., Wilquet, W.V., Drummond, R., Montmessin, F., Villard, E., 2008. HDO and H_2O vertical distributions and isotopic ratio in the Venus mesosphere by Solar Occultation at Infrared spectrometer on board Venus Express, J. Geophys. Res., 113, E00B22. https://doi.org/10.1029/2008JE003146

[3] Krasnopolsky, V.A., Belyaev, D.A., Gordon, I.E., Li, G., Rothman, L.S, 2013. Observations of D/H ratios in H_2O, HCl, and HF on Venus and new DCl and DF line strengths, Icarus 224, 57. https://doi.org/10.1016/j.icarus.2013.02.010

[4] Aoki, S., Vandaele, A.C., Daerden, F., Villanueva, G.L., Liuzzi, G., Thomas, I.R., Erwin, J.T., Trompet, L., Robert, S., Neary, L., Viscardy, S., Clancy, R.T., Smith, M.D., Lopez-Valverde, M.A., Hill, B., Ristic, B., Patel, M.R., Bellucci, G., Lopez-Moreno, J.-J., the NOMAD team, 2019. Water Vapor Vertical Profiles on Mars in Dust Storms Observed by TGO/NOMAD, Journal of Geophysical Research: Planets, Vol. 124, issue 12, 3482-3497. https://doi.org/10.1029/2019JE006109

[5] Crismani, M.M.J., Villanueva, G.L., Liuzzi, G., Smith, M.D., Knutsen, E.W., Daerden, F., Neary, L., Mumma, M.J. , Aoki, S., Trompet, L., Thomas, I.R., Ristic, B., Bellucci, G., Piccialli, A., Robert, S., Mahieux, A., Lopez Moreno, J.-J., Sindoni, G., Giuranna, M., Patel, M.R., Vandaele, A.C., 2021. A global and seasonal perspective of Martian water vapor from ExoMars/NOMAD, Journal of Geophysical Research: Planets, Vol. 126, issue 11, e2021JE006878. https://doi.org/10.1029/2021JE006878

[6] Aoki, S., Vandaele, A.C., Daerden, F., Villanueva, G.L., Liuzzi, G., Clancy, R.T., Lopez-Valverde, M.A., Brines, A., Thomas, I.R., Trompet, L., Erwin, J.T., Neary, L., Robert, S., Piccialli, A., Holmes, J.A., Patel, M.R., Yoshida, N., Whiteway, J., Smith, M.D., Ristic, B., Bellucci, G., Lopez-Moreno, J.J., Fedorova, A.A., 2022. Global Vertical Distribution of Water Vapor on Mars: Results From 3.5 Years of ExoMars-TGO/NOMAD Science Operations, Journal of Geophysical Research: Planets, Vol. 127, issue 9, e2022JE007231. https://doi.org/10.1029/2022JE007231

[7] Mahieux, A., Robert, S., Piccialli, A., Trompet, L., Vandaele, A.C., 2023. The SOIR/Venus Express species concentration and temperature database: CO_2, CO, H_2O, HDO, $H^{35}Cl$, $H^{37}Cl$, HF individual and mean profiles, Icarus, Vol. 405, issue , A115713. https://doi.org/10.1016/j.icarus.2023.115713

[8] Villanueva, G.L., Mumma, M.J., Novak, R.E., Käufl, H.U., Hartogh, P., Encrenaz, T., Tokunaga, A., Khayat, A., Smith, M.D., 2015. Strong water isotopic anomalies in the Martian atmosphere: Probing current and ancient reservoirs, Science, Vol 348, Issue 6231, pp. 218-221. https://doi.org/10.1126/science.aaa3630

[9] Vandaele, A.C., Korablev, O., Daerden, F., Aoki, S., Thomas, I.R., Altieri, F., … & Rodionov, D., 2019. Martian dust storm impact on atmospheric H_2O and D/H observed by ExoMars Trace Gas Orbiter, Nature, Vol. 568, issue 7753, 521-525. https://doi.org/10.1038/s41586-019-1097-3

[10] Villanueva, G.L., Liuzzi, G., Aoki, S., Stone, S.W., Brines, A., Thomas, I.R., ... & Vandaele, A.C., 2022. The deuterium isotopic ratio of water released from the Martian caps as measured with TGO/NOMAD, Geophysical Research Letters, Vol. 49, issue 12, e2022GL098161. https://doi.org/10.1029/2022GL098161

[11] Mahieux et al., 2024. Unexpected increase of the deuterium to hydrogen ratio in the Venus mesosphere, PNAS, in revision

[12] Régalia, L., Cousin, E., Gamache, R.R., Vispoel, B., Robert, S., Thomas, X., 2019. Laboratory measurements and calculations of line shape parameters of the H_2O–CO_2 collision system. J. Quant. Spectrosc. Radiat. Transf. 231, 126–135. https://doi.org/10.1016/j.jqsrt.2019.04.012

[13] Gamache, R.R., Neshyba, S.P., Plateaux, J.J., Barbe, A., Régalia, L., Pollack, J.B., 1995. CO_2-Broadening of Water-Vapor Lines. J. Mol. Spectrosc. 170, 131–151. https://doi.org/10.1006/jmsp.1995.1060

[14] Brown, L.R., Humphrey, C.M., Gamache, R.R., 2007. CO_2-broadened water in the pure rotation and v2 fundamental regions. J. Mol. Spectrosc. 246, 1–21. https://doi.org/10.1016/j.jms.2007.07.010

[15] Lavrentieva, N.N., Voronin, B.A., Fedorova, A.A., 2015. $H_2{}^{16}O$ line list for the study of atmospheres of Venus and Mars. Opt. Spectrosc. 118, 11–18. https://doi.org/10.1134/S0030400X15010178

[16] Gamache, R.R., Farese, M., Renaud, C.L., 2016. A spectral line list for water isotopologues in the 1100–4100cm^{-1} region for application to CO_2-rich planetary atmospheres. J. Mol. Spectrosc., New Visions of Spectroscopic Databases, Volume I 326, 144–150. https://doi.org/10.1016/j.jms.2015.09.001

[17] Borkov, Yu.G., Petrova, T.M., Solodov, A.M., Solodov, A.A., 2018. Measurements of the broadening and shift parameters of the water vapor spectral lines in the 10,100–10,800 cm^{-1} region induced by pressure of carbon dioxide. J. Mol. Spectrosc. 344, 39–45. https://doi.org/10.1016/j.jms.2017.10.010

[18] Deichuli, V.M., Petrova, T.M., Solodov, A.A., Solodov, A.M., 2022a. Broadening and Shift Coefficients of Water Absorption Lines Induced by Carbon Dioxide Pressure near 2.7 μm. Atmospheric Ocean. Opt. 35, 634–638. https://doi.org/10.1134/S1024856022060070

[19] Deichuli, V.M., Petrova, T.M., Solodov, A.M., Solodov, A.A., Fedorova, A.A., 2022b. Water vapor absorption line parameters in the 6760–7430 cm^{-1} region for application to CO_2-rich planetary atmosphere. J. Quant. Spectrosc. Radiat. Transf. 293, 108386. https://doi.org/10.1016/j.jqsrt.2022.108386

[20] Petrova, T.M., Solodov, A.M., Solodov, A.A., Deichuli, V.M., Lavrent'eva, N.N., Dudaryonok, A.S., 2023. Measurements and calculations of CO_2-broadening and shift coefficients of water vapor transitions in the 5150–5550 cm^{-1} spectral region. J. Quant. Spectrosc. Radiat. Transf. 311, 108757. https://doi.org/10.1016/j.jqsrt.2023.108757

[21] Devi, V. M., Benner, D. C., Sung, K., Crawford, T. J., Gamache, R.R., Renaud, C. L., Smith, M.-A.H., Mantz, A.W., Villanueva, G.L., 2017. Line parameters for CO_2 broadening in the ν_2 band of $HD_{16}O$. J. Quant. Spectrosc. Radiat. Transf. 187, 472-488. https://doi.org/10.1016/j.jqsrt.2016.10.004

[22] Devi, V. M., Benner, D. C., Sung, K., Crawford, T. J., Gamache, R.R., Renaud, C. L., Smith, M.-A.H., Mantz, A.W., Villanueva, G.L., 2017. Line parameters for CO_2- and self-broadening in the ν_1 band of $HD_{16}O$. J. Quant. Spectrosc. Radiat. Transf. 203, 133-157. https://doi.org/10.1016/j.jqsrt.2017.01.032

[23] Devi, V. M., Benner, D. C., Sung, K., Crawford, T. J., Gamache, R.R., Renaud, C. L., Smith, M.-A.H., Mantz, A.W., Villanueva, G.L., 2017. Line parameters for CO_2- and self-broadening in the ν_3 band of $HD_{16}O$. J. Quant. Spectrosc. Radiat. Transf. 203, 158-174. https://doi.org/10.1016/j.jqsrt.2017.02.020

[24] Gamache, R.R., Laraia, A.L., Lamouroux, J., 2011. Half-widths, their temperature dependence, and line shifts for the HDO–CO_2 collision system for applications to CO_2-rich planetary atmospheres. Icarus 213, 720-730. https://doi.org/10.1016/j.icarus.2011.03.021

[25] Plateaux, J.-J., Régalia, L., Boussin, C., Barbe, A., 2001. Multispectrum fitting technique for data recorded by Fourier transform spectrometer: application to N_2O and CH_3D. J. Quant. Spectrosc. Radiat. Transf. 68, 507–520. https://doi.org/10.1016/S0022-4073(00)00040-6

[26] Lyulin, O.M., 2015. Determination of spectral line parameters from several absorption spectra with the multispectrum fitting computer code. Atmospheric Ocean. Opt. 28, 487–495. https://doi.org/10.1134/S102485601506010X

[27] Birk, M., Wagner, G., 2012. Temperature-dependent air broadening of water in the 1250–1750 cm^{-1} range. J. Quant. Spectrosc. Radiat. Transf. 113, 889–928. https://doi.org/10.1134/S102485601506010X

[28] Gamache, R. R., Orphanos, N., Vispoel, B., Sung, K., Toon, G. C., 2023. Measurements of H_2O–O_2 line shape parameters and the determination of the intermolecular potential for modified complex Robert-Bonamy calculations. Molecular Physics. e2281592. https://doi.org/10.1080/00268976.2023.2281592

[29] Gordon, I.E., Rothman, L.S., Hargreaves, R.J., Hashemi, R., Karlovets, E.V., Skinner, F.M., Conway, E.K., Hill, C., Kochanov, R.V., Tan, Y., Wcisło, P., Finenko, A.A., Nelson, K., Bernath, P.F., Birk, M., Boudon, V., Campargue, A., Chance, K.V., Coustenis, A., Drouin, B.J., Flaud, J. –M., Gamache, R.R., Hodges, J.T., Jacquemart, D., Mlawer, E.J., Nikitin, A.V., Perevalov, V.I., Rotger, M., Tennyson, J., Toon, G.C., Tran, H., Tyuterev, V.G., Adkins, E.M., Baker, A., Barbe, A., Canè, E., Császár, A.G., Dudaryonok, A., Egorov, O., Fleisher, A.J., Fleurbaey, H., Foltynowicz, A., Furtenbacher, T., Harrison, J.J., Hartmann, J. –M., Horneman, V. –M., Huang, X., Karman, T., Karns, J., Kassi, S., Kleiner, I., Kofman, V., Kwabia–Tchana, F., Lavrentieva, N.N., Lee, T.J., Long, D.A., Lukashevskaya, A.A., Lyulin, O.M., Makhnev, V.Yu., Matt, W., Massie, S.T., Melosso, M., Mikhailenko, S.N., Mondelain, D., Müller, H.S.P., Naumenko, O.V., Perrin, A., Polyansky, O.L., Raddaoui, E., Raston, P.L., Reed, Z.D., Rey, M., Richard, C., Tóbiás, R., Sadiek, I., Schwenke, D.W., Starikova, E., Sung, K., Tamassia, F., Tashkun, S.A., Vander Auwera, J., Vasilenko, I.A., Vigasin, A.A., Villanueva, G.L., Vispoel, B., Wagner, G., Yachmenev, A., Yurchenko, S.N., 2022. The HITRAN2020 molecular spectroscopic database. J. Quant. Spectrosc. Radiat. Transf. 277, 107949. https://doi.org/10.1016/j.jqsrt.2021.107949

[30] Armstrong, B.H., 1967. Spectrum line profiles: The Voigt function. J. Quant. Spectrosc. Radiat. Transf. 7, 61–88. https ://doi.org/10.1016/0022-4073(67)90057-X

[31] Claveau, C., Henry, A., Lepère, M., Valentin, A., Hurtmans, D., 2002. Narrowing and Broadening Parameters for H_2O Lines in the ν_2 Band Perturbed by Nitrogen from Fourier Transform and Tunable Diode Laser Spectroscopy. J. Mol. Spectrosc. 212, 171–185. https://doi.org/10.1006/jmsp.2002.8539

[32] Lisak, D., Havey, D.K., Hodges, J.T., 2009. Spectroscopic line parameters of water vapor for rotation-vibration transitions near 7180 cm^{-1}. Phys. Rev. A 79, 052507. https://doi.org/10.1103/PhysRevA.79.052507

[33] Ngo, N.H., Tran, H., Gamache, R.R., Hartmann, J.M., 2012b. Pressure effects on water vapour lines: beyond the Voigt profile. Philos. Trans. R. Soc. Math. Phys. Eng. Sci. 370, 2495–2508. https://doi.org/10.1098/rsta.2011.0272

[34] Ngo, N.H., Lisak, D., Tran, H., Hartmann, J.-M., 2013. An isolated line-shape model to go beyond the Voigt profile in spectroscopic databases and radiative transfer codes. J. Quant. Spectrosc. Radiat. Transf. 129, 89–100. https://doi.org/10.1016/j.jqsrt.2013.05.034

[35] Rautian, S.G., Sobel'man, I.I., 1967. The effect of collisions on the Doppler broadening of spectral lines. Sov. Phys. Uspekhi 9, 701. https://doi.org/10.1070/PU1967v009n05ABEH003212

[36] Berman, P.R., 1972. Speed-dependent collisional width and shift parameters in spectral profiles. J. Quant. Spectrosc. Radiat. Transf. 12, 1331–1342. https://doi.org/10.1016/0022-4073(72)90189-6

[37] Pickett, H.M., 1980. Effects of velocity averaging on the shapes of absorption lines. J. Chem. Phys. 73, 6090–6094. https://doi.org/10.1063/1.440145

[38] Rohart, F., Mäder, H., Nicolaisen, H., 1994. Speed dependence of rotational relaxation induced by foreign gas collisions: Studies on CH_3F by millimeter wave coherent transients. J. Chem. Phys. 101, 6475–6486. https://doi.org/10.1063/1.468342

[39] Rohart, F., Ellendt, A., Kaghat, F., Mäder, H., 1997. Self and Polar Foreign Gas Line Broadening and Frequency Shifting of CH_3F: Effect of the Speed Dependence Observed by Millimeter-Wave Coherent Transients. J. Mol. Spectrosc. 185, 222–233. https://doi.org/10.1006/jmsp.1997.7395

[40] Rohart, F., Nguyen, L., Buldyreva, J., Colmont, J.-M., Wlodarczak, G., 2007. Lineshapes of the 172 and 602GHz rotational transitions of $HC^{15}N$. J. Mol. Spectrosc. 246, 213–227. https://doi.org/10.1016/j.jms.2007.09.009

[41] Rohart, F., Wlodarczak, G., Colmont, J.-M., Cazzoli, G., Dore, L., Puzzarini, C., 2008. Galatry versus speed-dependent Voigt profiles for millimeter lines of O_3 in collision with N_2 and O_2. J. Mol. Spectrosc., Special issue dedicated to the pioneering work of Drs. Edward A. Cohen and Herbert M. Pickett on spectroscopy relevant to the Earth's atmosphere and astrophysics 251, 282–292. https://doi.org/10.1016/j.jms.2008.03.005

[42] Lance, B., Blanquet, G., Walrand, J., Bouanich, J.-P., 1997. On the Speed-Dependent Hard Collision Lineshape Models: Application to C_2H_2 Perturbed by Xe. J. Mol. Spectrosc. 185, 262–271. https://doi.org/10.1006/jmsp.1997.7385

[43] Ngo, N.H., Ibrahim, N., Landsheere, X., Tran, H., Chelin, P., Schwell, M., Hartmann, J.-M., 2012a. Intensities and shapes of H_2O lines in the near-infrared by tunable diode laser spectroscopy. J. Quant. Spectrosc. Radiat. Transf., Three Leaders in Spectroscopy 113, 870–877. https://doi.org/10.1016/j.jqsrt.2011.12.007

[44] Tran, H., Ngo, N.H., Hartmann, J.-M., 2013. Efficient computation of some speed-dependent isolated line profiles. J. Quant. Spectrosc. Radiat. Transf. 129, 199–203. https://doi.org/10.1016/j.jqsrt.2013.06.015

[45] Dicke, R.H., 1953. The Effect of Collisions upon the Doppler Width of Spectral Lines. Phys. Rev. 89, 472–473. https://doi.org/10.1103/PhysRev.89.472

[46] Tinetti, G., Haswell, C., Leconte, J., Lagage, P.-O., MicelaSarkar, G., Min, M., Testi, L., Turrini, D., Vandenbussche, B., Osorio, M.R. Z., Eccleston, P., Swain, M., ESA Study Team, Ariel Mission Consortium, Griffin, M. , Hargrave, P. and Sarkar, S., 2020. Ariel: Atmospheric Remote-sensing Infrared Exoplanet Large-survey - enabling planetary science across light-years. Definition study report. European Space Agency. https://www.cosmos.esa.int/documents/1783156/3267291/Ariel_RedBook_Nov2020.pdf/

[47] Chubb, K.L., Robert, S., Sousa-Silva, C., Yurchenko, S.N., Allard, N.F., Boudon, V., ... & Zingales, T., 2024. Data availability and requirements relevant for the Ariel space mission and other exoplanet atmosphere applications, submitted to RASTI. https://doi.org/10.48550/arXiv.2404.02188

[48] Straume et al., 2023. EnVision, Understanding why Earth's closest neighbour is so different, ESA Red Book. https://www.cosmos.esa.int/documents/10892653/0/EnVision+Red+Book_ESA-SCI-DIR-RP-003+(1).pdf

Table captions

Table 1. Experimental conditions for the FT-IR spectrometer for measurements in 2.7 µm region, i.e. around 3704 cm^{-1}.

Table 2. Experimental conditions of the four H_2O – CO_2 spectra for the 2.7 µm region. The path length was 826.2 cm, and the aperture radius was 0.85 mm.

Table 3. Comparison between measured and fitted H_2O partial pressures of H_2O – CO_2 spectra for the "injection" series in 2.7 µm region. The relative deviation was calculated as follows (fitted pressure - measured pressure)/measured pressure.

Table 4. Profiles used for the H_2O – CO_2 collision system. The parameters are described as follows: Γ_0 the pressure-induced broadening coefficient ($cm^{-1}.atm^{-1}$), Δ_0 the pressure-induced shift coefficient ($cm^{-1}.atm^{-1}$), Γ_2 the speed-dependence of the pressure-induced broadening coefficient ($cm^{-1}.atm^{-1}$), Δ_2 the speed-dependence of the pressure-induced shift coefficient ($cm^{-1}.atm^{-1}$), ν_{VC} the frequency rate of velocity-changing collisions ($cm^{-1}.atm^{-1}$).

Figure captions

Figure 1. Example of H_2O broadened by CO_2 spectra in 2.7 µm region, with a zoom around 3957 cm^{-1}.

Figure 2. Fit residuals without (left panel) and with (right panel) water vapor partial pressure correction (Table 3) for one transition centered at 3421.74 cm^{-1} using a Voigt profile.

Figure 3. Comparison for 20 ν_3 transitions of experimental CO_2 broadening coefficients from [12] and MCRB calculations performed for our previous study [12] with *S2023* using a Voigt profile with and without the water vapor partial pressure correction. The uncertainties are the numerical errors provided by the multi-spectrum fitting procedure at 3-sigma.

Figure 4. Example in 2.7 µm region of H_2O broadened by CO_2 spectra fits using different line profiles and their 100 x (Obs.-Calc.) residuals.

Figure 5. Comparison between our CO_2 broadening coefficients and their speed dependence (*S2023* with H_2O partial pressure correction) with those of Deichuli *et al*., 2022a [18]. The uncertainties came from numerical errors provided by the multi-spectrum fitting procedure at 3-sigma.

(All figures in color)

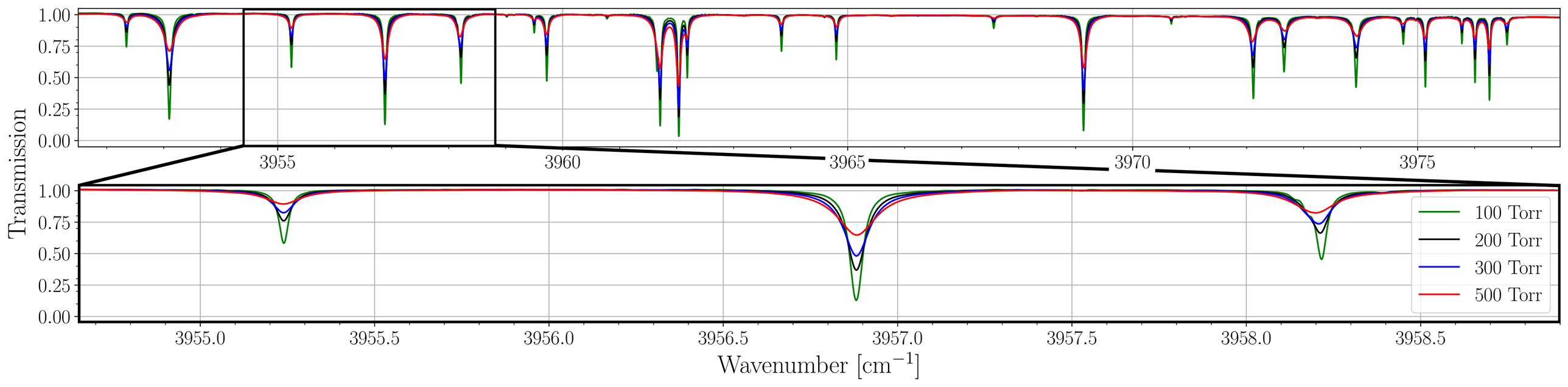
Transmission
1.00
0.75
0.50
0.25
0.00
3955
3960
3965
3970
3975
3955.0
3955.5
3956.0
3956.5
3957.0
3957.5
3958.0
3958.5
Wavenumber [cm^{-1}]
100 Torr
200 Torr
300 Torr
500 Torr

Transmission

observed
calculated (Voigt)

100 Torr
200 Torr
300 Torr
500 Torr

100 × (Obs.-Calc.)

Wavenumber [cm^{-1}]

MCRB calculations from [12]
S2023 without corrected pressure
S2023 with corrected pressure
Régalia *et al.* 2019 [12]

CO_2-broadened half-widths of H_2O [cm^{-1} atm^{-1}]

0.16
0.14
0.12
0.10
0.08
0.06

20
40
60
80
100
120

J"×(J"+1)+Ka"−Kc"+1

Transmission
Voigt
Rautian
qSDV
qSDR
100 Torr
200 Torr
300 Torr
500 Torr
Wavenumber [cm^{-1}]

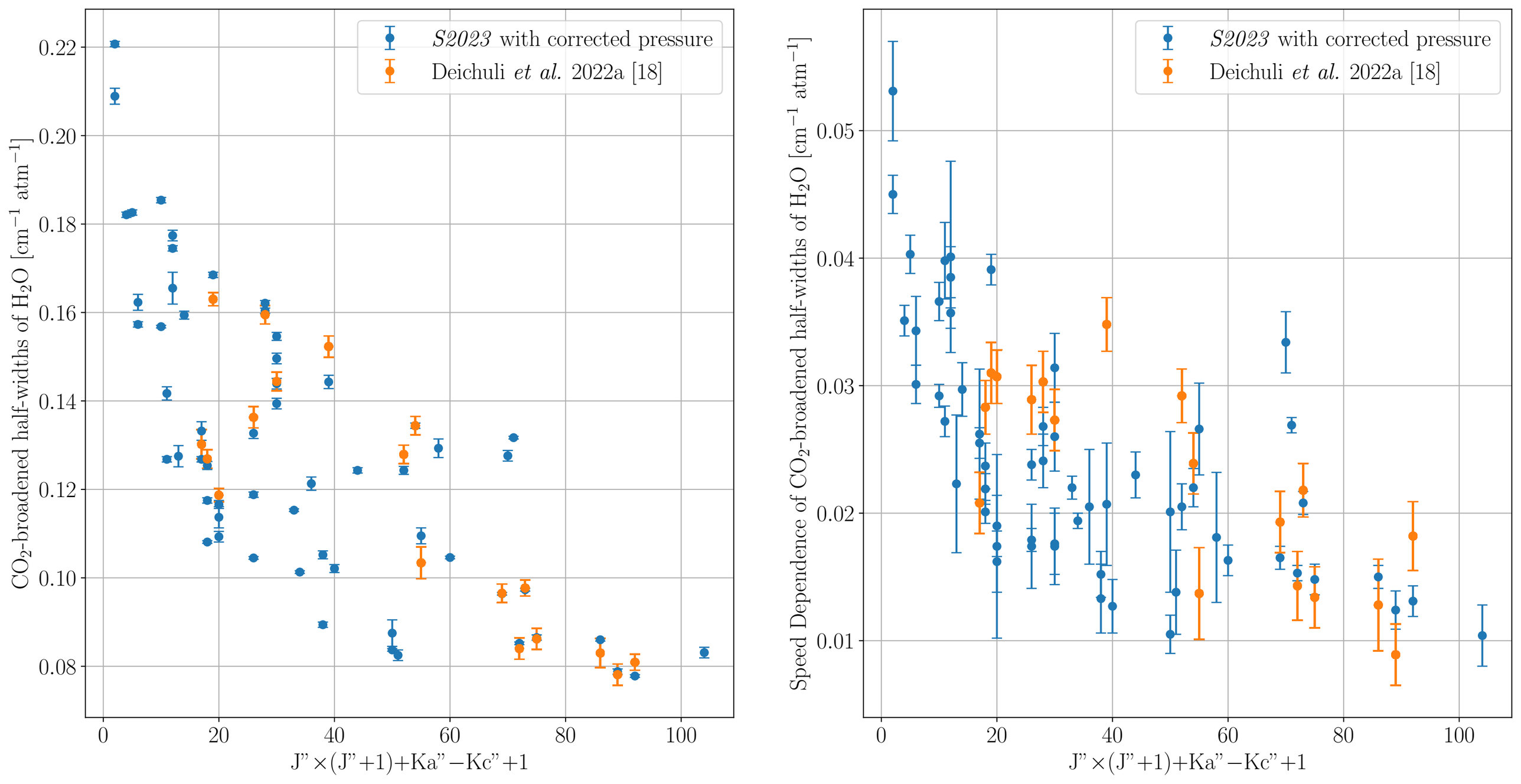
S2023 with corrected pressure
Deichuli et al. 2022a [18]
CO2-broadened half-widths of H2O [cm−1 atm−1]
Speed Dependence of CO2-broadened half-widths of H2O [cm−1 atm−1]
J"×(J"+1)+Ka"−Kc"+1
0.22
0.20
0.18
0.16
0.14
0.12
0.10
0.08
0.05
0.04
0.03
0.02
0.01
0
20
40
60
80
100

Table 1

Source	Globar SiC
Tension	24 V
Intensity	3.28 A
Iris radius	0.85 mm
Focal length	41.8 cm
Modulation frequency	40 kHz
Optical filter	Band pass 3060 – 4370 cm^{-1}
Beam splitter	CaF_2
Detector	InSb, 77 K

Table 2

Total pressure [Torr]	**MDP [cm]**	**Spectral resolution [cm^{-1}]**	**Temperature [K]**
99.4	56.25	0.016	291.8
200.4	50.00	0.018	291.7
300.1	45.00	0.020	291.8
500.6	40.90	0.022	291.8

Table 3

Total pressure [Torr]	**Measured P(H_2O) [Torr]**	**Fitted P(H_2O) [Torr]**	**Relative deviation**
99.4	1.465	1.422	-2.9%
200.4	1.465	1.419	-3.1%
300.1	1.465	1.421	-3.0%
500.6	1.465	1.421	-3.0%

Table 4

Profile	**Parameters**
VP	Γ_0, Δ_0
RP	Γ_0, Δ_0, v_{VC}
qSDVP	Γ_0, Δ_0, Γ_2, Δ_2
qSDRP	Γ_0, Δ_0, Γ_2, Δ_2, v_{VC}